Event-Related Potential Markers of Subject Cognitive Decline and Mild Cognitive Impairment during a sustained visuo-attentive task

A. A. Vergani[1,2], S. Mazzeo[3,4], V. Moschini[4], R. Burali[3], M. Lassi[1,2], L. G. Amato[1,2], J. Carpaneto[1,2], G. Salvestrini[3], C. Fabbiani[3,4], G. Giacomucci[4], C. Morinelli[4], F. Emiliani[4], M. Scarpino[3], S. Bagnoli[4], A. Ingannato[4], B. Nacmias[3,4], S. Padiglioni[5], S. Sorbi[3,4], V. Bessi[4], A. Grippo[3], A. Mazzoni[1,2]*

* Corresponding author: alberto.mazzoni@santannapisa.it

[1]The BioRobotics Institute, Sant'Anna School of Advanced Studies, Pisa, Italy
[2]Department of Excellence in Robotics and AI, Sant'Anna School of Advanced Studies, Pisa, Italy
[3]IRCSS Fondazione Don Carlo Gnocchi, Florence, Italy
[4]Department of Neuroscience, Psychology, Drug Research and Child Health, Azienda Ospedaliero-universitaria Careggi, Florence, Italy
[5] Research and Innovation Centre for Dementia-CRIDEM, Azienda Ospedaliero-universitaria Careggi, Florence, Italy

Abstract

INTRODUCTION. Subjective cognitive decline (SCD), mild cognitive impairment (MCI), or severe Alzheimer's disease stages are still lacking clear electrophysiological correlates.

METHODS. In 145 subjects (86 SCD, 40 MCI, and 19 healthy subjects (HS)), we analysed event-related potentials observed during a sustained visual attention task, aiming to distinguish biomarkers associated with group conditions and performance.

RESULTS. We observed distinct patterns among group conditions in the occipital P1 and N1 components during the stimulus encoding phase, as well as in the central P3 component during the stimulus decision phase. The order of ERP components was non-monotonic, indicating a closer resemblance between MCI and HS. ERP features from occipital channels exhibited greater differences between SCD and MCI. Task performance was significantly enhanced in the central channels during the decision phase.

DISCUSSION. Those results support evidence of early stage, neural anomalies linked to visuo-attentive alterations in cognitive decline as candidate EEG biomarkers.

Research in context

THE SYSTEMATIC REVIEW. The researchers examined existing literature by referring to conventional sources like PubMed, Scopus, and Google Scholar. Keywords used: e.g., "EEG & Dementia"; "Visual Evoked Potential & SCD or MCI". References are properly cited and almost half of them are from the last ten years.

THE INTERPRETATION. Results proposed early dynamics of visual processing ERP being insightful biomarkers for SCD and MCI patients. Those components reflect evoked potential patterns, suggesting the power of few milliseconds in being informative about the underlying neural dysfunctionalities associated with visuo-attentive mechanisms.

FUTURE DIRECTIONS. We enrolled 100+ subjects. By even expanding the sample size and conducting follow-up assessments, we aim to assess the extracted ERP features, as well as by training and testing machine learning algorithms. The goal is to support clinical decision-making, and to prioritise patients with an abnormal neural signal over manifest cognitive symptomatology, tracking the cognitive decline trajectory effectively.

Background

Neurocognitive disorders affect 6-50 million people worldwide, with prevalence doubling every five years, particularly among those aged 50-80. This trend poses a significant societal burden, with various factors contributing to dementia, including neurological, systemic, and psychiatric conditions. Alzheimer's disease (AD) is the most prevalent cause of neurocognitive decline.

AD involves the accumulation of beta-amyloid plaques and neurofibrillary tangles, leading to neurodegeneration and cognitive decline, eventually resulting in dementia. This process unfolds over decades, with amyloid buildup occurring years before symptoms. Stages range from subtle cognitive changes to full-blown dementia. The initial stage, Subjective Cognitive Decline (SCD), involves self-reported cognitive decline while performance on standardized tests remains within the normal range when adjusted for age, sex, and education (1).

Mild Cognitive Impairment (MCI) occurs when pathological scores on neuropsychological tests are present without a significant impact on daily life activities. It serves as a transitional stage between normal aging and the more severe cognitive decline seen in dementia.

In the realm of dementia research, SCD and MCI hold paramount significance as they fall within the spectrum of AD. Patients affected by these conditions present an opportunity for intervention with recently developed Disease-Modifying Therapies (DMTs) approved for AD (2,3). Indeed, it is widely acknowledged that DMTs should be administered during the early stages of the disease, prior to the onset of neurodegeneration (4).

Seeking reliable biomarkers for early AD diagnosis is crucial. Common biomarkers like MRI, FDG-PET, and CSF are invasive and not widely available. Hence, researchers explore accessible options, with EEG showing promise (5). Nevertheless, despite these efforts, only a limited number of studies have delved into this promising avenue (e.g., biomarking conditions as SCD against MCI (6,7), MCI against AD (8), across CSF (9) and ApoE ε-4 allele (10))

Additionally, in dementia EEG studies, sensory event-related potentials are examined (e.g., auditory (11) and visual (12–14)). Specifically, visual event-related potentials suggest a compelling hypothesis about brain alterations in the visual system that could help detect early structural changes linked to anomalies in ERPs (15–17). For example, by recording EEG during a visuo-memory task, Waninger et al (18) found amplitude suppression of late positive potentials (~400ms) in MCI against healthy subjects over right occipital and temporal channels. Other studies enquired early phase of visual processing as the encoding of stimulus: Krasodomska et al (19) found N95 wave dynamics alterations in AD, as other colleagues in last decays detect visual evoked potential anomalies in dementia patients (20,21). Hence, an unresolved critical aspect is how visual alterations manifest across various stages of cognitive decline.

In this study, we aimed to uncover EEG correlates of a sustained visuo-attentive task paradigm. Our goal was to quantitatively characterize patients with SCD and MCI, thereby enhancing our understanding of electrophysiology in the dementia continuum.

Methods

The protocol of the PREVIEW project (ClinicalTrials.gov Identifier: NCT05569083) has been published previously (22). In brief, PREVIEW is a longitudinal study on Subjective Cognitive Decline started in October 2020 with the aim to identify features derived from easily accessible, cost-effective and non-invasive assessment to accurately detect SCD patients who will

progress to AD dementia. All participants were collected in agree with the Declaration of Helsinki and with the ethical standards of the Committee on Human Experimentation of Careggi University Hospital (Florence, Italy). The study was approved by the local Institutional Review Board (reference 15691oss).

Participants

We enrolled 145 individuals (92F), including 86 SCD patients (59F), 40 MCI patients (25F), and 19 age-matched healthy individuals (8F). All participants underwent thorough family and clinical history evaluations, neurological examinations, extensive neuropsychological assessments, premorbid intelligence estimation, and depression evaluations.

The following inclusion criteria were adopted: satisfied criteria for SCD (23) or MCI (24); Mini Mental State Examination (MMSE) score >24, corrected for age and education; normal functioning on the Activities of Daily Living (ADL) and the Instrumental Activities of Daily Living (IADL) scales unsatisfied criteria for AD diagnosis according to National Institute on Aging-Alzheimer's Association (NIA-AA) criteria (25). Exclusion criteria were history of head injury, current neurological and/or systemic disease, symptoms of psychosis, major depression, substance use disorder; complete data loss of patients' follow-up; use of any medication with known effects on EEG oscillations, such as benzodiazepines or antiepileptic drugs. In addition, an exclusion criterion was for subjects with outliers (>3.5 sigma) for multiple ERP features (see Methods).

A subset of 44 patients underwent CSF collection for assessment of $A\beta_{42}$, $A\beta_{42}/A\beta_{40}$, total-tau (t-tau) and phosphorylated-tau (p-tau). Among these, 44 patients (25 SCD, 19 MCI) also underwent cerebral amyloid-PET. Normal values for CSF biomarkers were: $A\beta_{42}$>670 pg/ml, $A\beta_{42}/A\beta_{40}$ ratio>0.062, t-tau<400 pg/ml and p-tau<60 pg/ml (26). Methods used CSF collection, biomarker analysis, and amyloid-PET acquisition and rating are described in further detail elsewhere (22,27). Patients who underwent AD biomarker assessment, were classified as A+ if at least one of the amyloid biomarkers (CSF $A\beta_{42}$, $A\beta_{42}/A\beta_{40}$ or amyloid PET) indicated the presence of Aβ pathology, and as A- if none of the biomarkers indicated the presence of Aβ pathology. In cases where there were conflicting results between CSF and Amyloid PET, only the pathological result was considered. Patients were classified as T+ or T- based on whether their CSF p-tau concentrations were higher or lower than the cut-off value, respectively. Similarly, patients were classified as N+ or N- depending on whether their t-tau concentrations were higher or lower than the cut-off value. Using this initial classification, we applied the NIA-AA Research Framework (28) to define the following groups: ATN 0 (28 of 44; 17 SCD + 11 MCI): normal AD biomarkers (A-/T-/N-) and non-AD pathologic change (A-/T+/N-, A-/T-/N+, and A-/T+/N+); ATN 1 (6 of 44; 4 SCD + 2 MCI): Alzheimer's pathologic change (A+/T-/N- and A+/T-/N+); ATN 2 (10 of 44; 4 SCD + 6 MCI): AD (including A+/T+/N- and A+/T+/N+).

Visuo-attentive task

The 3-Choice Vigilance Test (3CVT) requires identifying a target shape (upward triangle) among two distractor shapes (downward triangle and diamond) (29) (Fig1A). Shapes are shown for 0.2 seconds with varied interstimulus intervals in the 20-minute task. Participants press left for targets (70%) and right for distractors (30%) (Fig1B/C). Performance is evaluated using reaction time, accuracy, and F-Measure, considering both reaction time and accuracy (29).

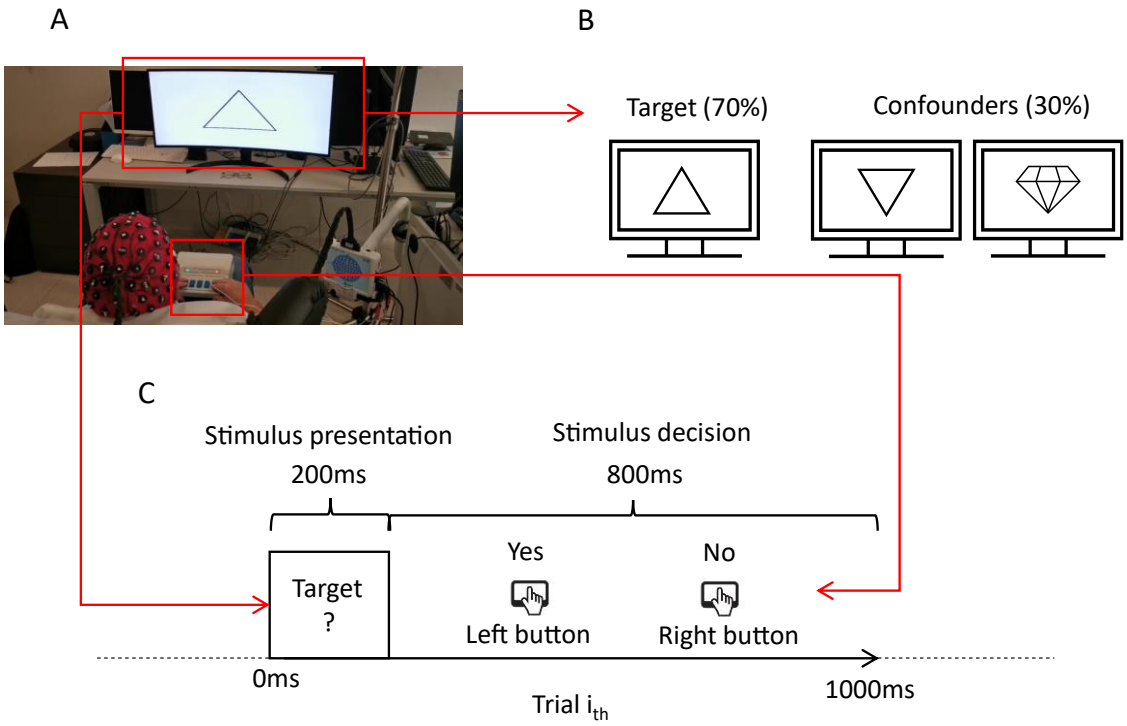

Figure 1. 3CVT experimental paradigm. Panel A shows both experiment and EEG settings while subjects must push left button in the presence of the target stimulus, while must push right button in the presence of confound stimuli. Panel B shows the target stimulus (upward triangle) and the confounders (downward triangle and diamond). Target stimulus is presented 70% of the time, while non-target stimuli are presented 30% of the time. Panel C shows an exemplificative trial temporal structure with 200ms of stimulus presentation and 800ms for making the decision.

EEG devices

EEG data were collected from eligible subjects at IRCCS Don Gnocchi (Florence, Italy) using the 64-channel Galileo-NT system (E.B. Neuro S.p.a.). Sensor placement followed the extended 10/20 system (30). Signals were recorded unipolarly at 512 Hz. Electrode impedances were maintained between 7 and 10 KOhm; if exceeded, electrodes were readjusted, and affected segments were removed.

EEG preprocessing and computation

EEG processing included band-pass filtering (1-45 Hz), noisy channel interpolation, average re-referencing, and artefactual component exclusion via ICA. Trials lasted 1000 ms, with 200 ms for stimulus presentation and 800 ms for response. ERPs were epoch-aligned with correct responses to the target stimulus, segmented from 0 to 750 ms with a -100 ms baseline. Average EEG signals from occipital (PO7, PO8, O1, Oz, O2) and central channels (FC1, FCz, FC2, C1, Cz, C2) were computed for encoding and decision-making analysis, respectively.

ERP components definitions

We examined occipital and central channel signals, identifying canonical components. Occipital channels revealed P1 (60-80ms) and N1 (110-170ms). Central channels showed P2 (300-500ms) and P3 (470-650ms), also called P300 (31) and Late Positive Potentials (LPP) (32) respectively. P2 and P3 together formed Extended Central Potential, named based on voltage polarity (P=positive, N=negative) and appearance order.

Neural features computations

We extracted neural features from defined ERP components, including voltage peaks, latencies, and integrals. To explore visual processes' impact on cognitive decline and understand visual decision-making, we introduced a seed-based correlation measure using Spearman rank-order correlation coefficient (33–35). Two seeds, from occipital and central channels, were utilized to compute correlations within encoding (0-200ms) and decision (200-750ms) time windows, yielding median values representing overall EEG signal relationships.

Patients' descriptors

Patients underwent an extensive neuropsychological examination (see specific references in (22)), including global measurements (MMSE), attention (TMTA, TMTB, TMTAB, visual search, MFTC FR, MFTC Time), executive function (TMT B), and premorbid intelligence estimation (TIB). Personality traits were assessed using the BFFQ, and participation in intellectual, social, and physical activities was evaluated. Patient descriptors also included performance on the 3CVT task (accuracy, reaction time, and F-Measure; see detailed equations in (18)).

Computational notes

Non-parametric analysis was employed, with statistics presented as mean values and 95% confidence intervals (CI). Group comparisons utilized the Kruskal-Wallis H test, with post-hoc analysis conducted using the Mann-Whitney U test. Differences in ERP voltage dynamics were assessed by comparing voltage values at each time point across channels (central or occipital). Effect size was measured using the eta squared index, and p-values were corrected using Bonferroni correction for multiple comparisons. Data preprocessing utilized EEGLAB (36), while postprocessing and visualization were performed using Python libraries. Scripts and data are available upon request.

Results

Relation between medical scales and task performance results

Medical scale results revealed significant differences in several patient descriptors between the two diagnostic groups (details in Tab1). Patients with SCD were younger and more educated than those with MCI. In neuropsychological assessments, SCD outperformed MCI in global cognition (MMSE) and premorbid intelligence (TIB). While SCD performed better than MCI in visuo-attentive tests, results were not statistically significant. SCD patients also exhibited higher emotional stability, extraversion, agreeableness, and openness compared to MCI patients. Additionally, SCD patients were more engaged in mental, social, and physical activities compared to MCI patients.

Group analysis of task performance showed significant differences for accuracy (H=7.33e+02; p=2.42e-03) and F-Meausure (H=6.29.50e+02; p=7.04e-03), but not for reaction time (H=0.33+e1; p=5.48e-01; see Fig2A)). Post-hoc analysis showed significant differences in accuracy (Fig2B) between MCI and SCD (U=2.3e+03; p=1.0e-03) and between MCI and HS (U=2.09e+03; p=1.7e-02), but not between SCD and HS (U=7.3e+02 with p=8.4e-1). Post-hoc analysis of F-Measure (Fig2C) showed significant difference between MCI and SCD (U=2.2e+03; p=2.20e-02) and between MCI and HS (U=1.86e+02; p=5.00e-03; Fig2C), but not between SCD and HS (U=6.28e+02; p=3.53e-01).

Table 1 Task performance and medical scale results. Values regarded features as 3CVT behaviour performance, clinical scales, demography, leisure time, personality traits scales and neuropsychological scales of visuo-attention. P-value in bold is <0.05. Features values are indicated with mean and 95% confidence level (CI). Abbreviations: H is the Kruskal-Wallis statistics; Eta-squared is the statistics effect size; HS, healthy controls; SCD, subject cognitive decline; MCI, mild cognitive impairment.

Class	Feature	HS (Mean & CI)	SCD (Mean & CI)	MCI (Mean & CI)	H	p-value	Eta-squared
3CVT Performances	F-Measure [a.u.]	0.91 (0.90, 0.93)	0.89 (0.88, 0.90)	0.87 (0.85, 0.89)	6.29E+02	**7.05E-03**	7.80E-02
3CVT Performances	Accuracy [%]	95.39 (93.92, 96.86)	94.38 (93.30, 95.47)	90.53 (88.27, 92.79)	7.33E+02	**2.42E-03**	9.10E-02
3CVT Performances	Reaction Time [s]	0.45 (0.41, 0.48)	0.47 (0.45, 0.49)	0.49 (0.46, 0.52)	3.40E+00	5.49E-01	2.30E-02
Clinical	Age at onset of symptoms	-	55.97 (53.91, 58.02)	62.92 (59.67, 66.18)	1.21E+01	**1.48E-03**	8.90E-02
Clinical	TIB [a.u.]	-	113.71 (112.94, 114.49)	108.38 (103.74, 113.01)	7.54E+00	**1.81E-02**	5.70E-02
Clinical	MMSE [a.u.]	14.95 (13.42, 16.48)	27.94 (27.53, 28.36)	27.61 (26.06, 29.17)	1.63E+03	**7.13E-12**	2.72E-01
Demography	Education [years]	29.15 (28.65, 29.66)	13.73 (13.00, 14.46)	10.80 (9.55, 12.05)	0.00E+00	**6.13E-14**	3.03E-01
Demography	Age [Years]	-	65.42 (63.41, 67.42)	72.42 (69.82, 75.03)	1.42E+01	**3.22E-04**	1.03E-01
Leasure Time	Mental [a.u.]	-	19.09 (18.26, 19.91)	15.55 (13.96, 17.14)	2.00E+01	**2.36E-05**	1.39E-01
Leasure Time	Social [a.u.]	-	9.21 (8.49, 9.94)	7.40 (6.61, 8.19)	1.71E+01	**1.06E-04**	1.21E-01
Leasure Time	Physical [a.u.]	-	6.85 (6.24, 7.47)	5.52 (4.91, 6.12)	1.35E+01	**7.33E-04**	9.80E-02
Psychological	Openness of mind [a.u.]	-	47.48 (45.88, 49.07)	40.40 (38.49, 42.31)	2.22E+01	**1.22E-05**	1.52E-01
Psychological	Emotive stability [a.u.]	-	49.52 (47.77, 51.27)	48.30 (45.96, 50.64)	7.47E+00	**3.14E-02**	5.70E-02
Psychological	Agreeableness [a.u.]	-	51.95 (50.17, 53.74)	46.65 (44.82, 48.48)	2.74E+01	**8.25E-07**	1.81E-01
Psychological	Extraversion [a.u.]	-	46.70 (45.34, 48.06)	42.85 (40.98, 44.72)	2.24E+01	**1.11E-05**	1.53E-01
Psychological	Conscientiousness [a.u.]	-	48.53 (46.66, 50.41)	47.00 (44.84, 49.16)	4.66E+00	1.54E-01	3.60E-02
Visuo-Attentive	MFTC Time [s]	-	69.94 (64.43, 75.45)	74.22 (66.64, 81.81)	2.55E+00	7.73E-01	2.00E-02
Visuo-Attentive	MFTC FR [a.u.]	-	0.24 (0.00, 0.49)	2.42 (-1.93, 6.78)	9.11E-01	8.46E-01	7.00E-03
Visuo-Attentive	MFTC [a.u.]	-	97.73 (97.15, 98.32)	94.38 (89.56, 99.19)	4.43E+00	2.47E-01	3.50E-02
Visuo-Attentive	TMT AB [a.u.]	-	37.63 (29.98, 45.28)	47.75 (36.18, 59.32)	2.89E+00	6.24E-01	2.30E-02
Visuo-Attentive	TMT B [a.u.]	-	66.51 (56.79, 76.23)	79.38 (63.82, 94.93)	2.48E+00	8.06E-01	2.00E-02
Visuo-Attentive	TMT A [a.u.]	-	30.56 (27.36, 33.76)	44.67 (29.74, 59.61)	3.92E+00	3.34E-01	3.10E-02
Visuo-Attentive	Visual search [a.u.]	-	48.86 (47.47, 50.26)	45.96 (43.56, 48.37)	4.81E+00	1.98E-01	3.70E-02

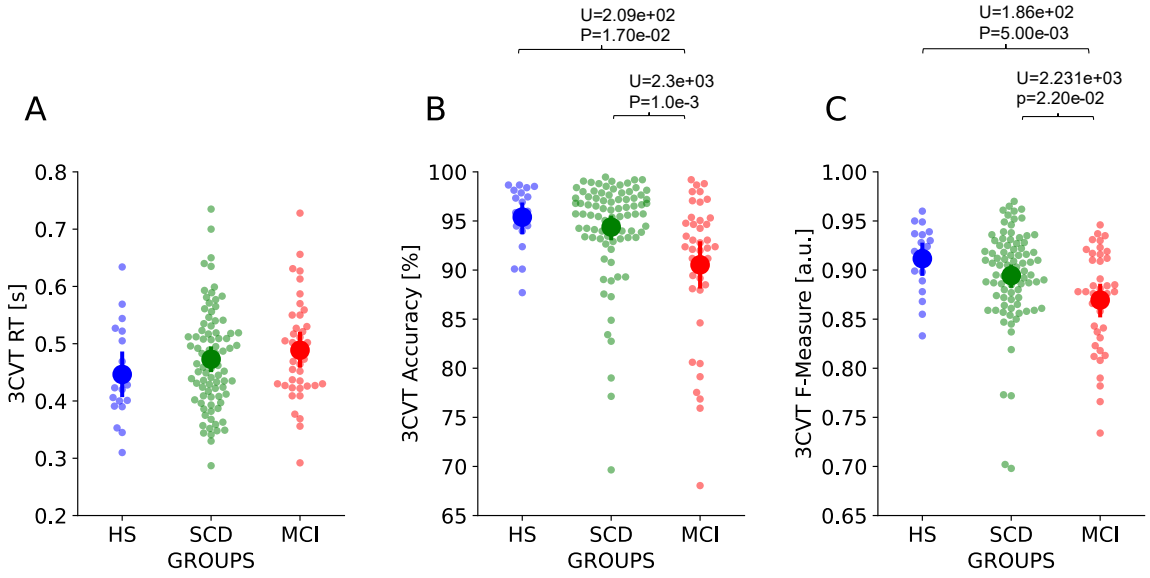

Figure 2. Task performance features. Panel A: reaction time stratified by groups. Panel B: accuracy values stratified by groups. Panel C: F-Measure stratified by groups. Small dots are subject specific values, while the big dot for each group is the mean value. Reported U statistics are significative (p<0.05). Colour code: SCD patients (86) are in green, MCI (40) in red and healthy subjects (19) in blue. Abbreviations: HS, healthy controls; SCD, subject cognitive decline; MCI, mild cognitive impairment).

ERPs revealed precise temporal anomalies in occipito-central channels

ERPs recorded in central and occipital channels exhibited significant group differences (Fig3). Decision speed representation (Fig3A) explicitly showed that reaction time aligned with cognitive decline ordering. During the decision phase (Fig3B), significant temporal differences (p<0.01) in the late window (>400ms) indicated prolonged attenuation (>100ms) of the P3 component in SCDs and MCIs compared to HSs. In the encoding phase (Fig3C), significant temporal differences (p<0.01) were observed at the P1 and N1 canonical deflections, showing attenuation of P1 in SCDs compared to MCI and HS, and overall attenuation of N1 in SCDs and MCIs compared to controls.

Significant temporal windows (violet lines in Fig3B/C) were identified for ERP component peaks and integrals extraction. Non-parametric seed-to-scalp correlations based on occipital and central seeds were computed. Group analysis (see detailed statistics in Tab2; single-feature outliers excluded) showed significant differences in occipital regions for N1 and P1 component peaks and integrals, and in central regions for P3 component peaks and integrals. Occipital seed-based correlations exhibited significant group differences, while central seed-based correlations did not.

Post-hoc analyses of significative features revealed that occipital P1 peak (Fig3D) was statistically different between SCD and MCI (U=1.109e+03; p=9.000e-03) and between SCD and HS (U=4.780e+02; p=2.300e-02), but not between MCI and HS (U=3.520e+02; p=8.697e-01); occipital N1 peak (Fig3E) between was not different between SCD and MCI (U=2.165e+03; p=5.900e-02) and between MCI and HS (U=5.100e+02; p=1.070e-01), but was statistically different between SCD and HS (U=1.230e+03; p=2.000e-03); central P3 integral (Fig3F) was statistically different between SCD and HS (U=4.380e+02; p=6.000e-03), but not between SCD and MCI (U=1.300e+03; p=1.640e-01) and between MCI and HS (U=2.450e+02; p=1.150e-01); occipital seed based correlation (Fig3G) was statistically different between SCD and MCI (U=2.290e+03; p=3.000e-03), but not between MCI and HS (U=3.530e+02; p=9.130e-01) and between SCD and HS (U=9.980e+02; p=1.020e-01); occipital N1 integral was statistically different between SCD and HS (U=4.460e+02; p=6.000e-03), but not between SCD and MCI (U=1.343e+03; p=1.450e-01) and between MCI and HS (U=2.590e+02; p=1.520e-01); occipital P1 integral was statistically different between SCD and MCI (U=1.129e+03; p=1.000e-02) and between SCD and HS (U=5.140e+02; p=4.800e-02), but not between MCI and HS (U=3.790e+02; p=9.510e-01); central P3 peak was statistically different SCD and HS (U=4.510e+02; p=8.000e-03), but not between SCD and MCI (U=1.335e+03; p=2.490e-01) and between MCI and HS (U=2.630e+02; p=2.290e-01).

Occipital seed scalp correlation (Fig3G) showed average topographic features: high anticorrelation values (~ -1) suggested occipito-frontal dipole effect, while low anti-correlation (~ -0.5) indicated more centralized scalp activation. ERP component features displayed non-monotonic ordering between groups (Fig3D-G), highlighting SCD as a distinct group compared to MCI and HS.

ERP dynamics stratified by ATN classification in patients

We examined ERP correlates in patients stratified by the ATN marker. No significant differences were found in canonical components in central and occipital channel groups (S-Fig1). However, when crossing diagnostic categories with ATN classes, SCD-ATN1 patients displayed an abnormal negative flection centred at 200ms in central channels (S-Fig2). In contrast, MCI-ATN2 patients showed suppression of central P3 potential around 580ms (S-Fig3). ATN taxonomy mainly correlates with central channels. Fragmentary subgroup numbering (pie plots in S-Fig2 and S-Fig3) lacks statistical power for further analysis.

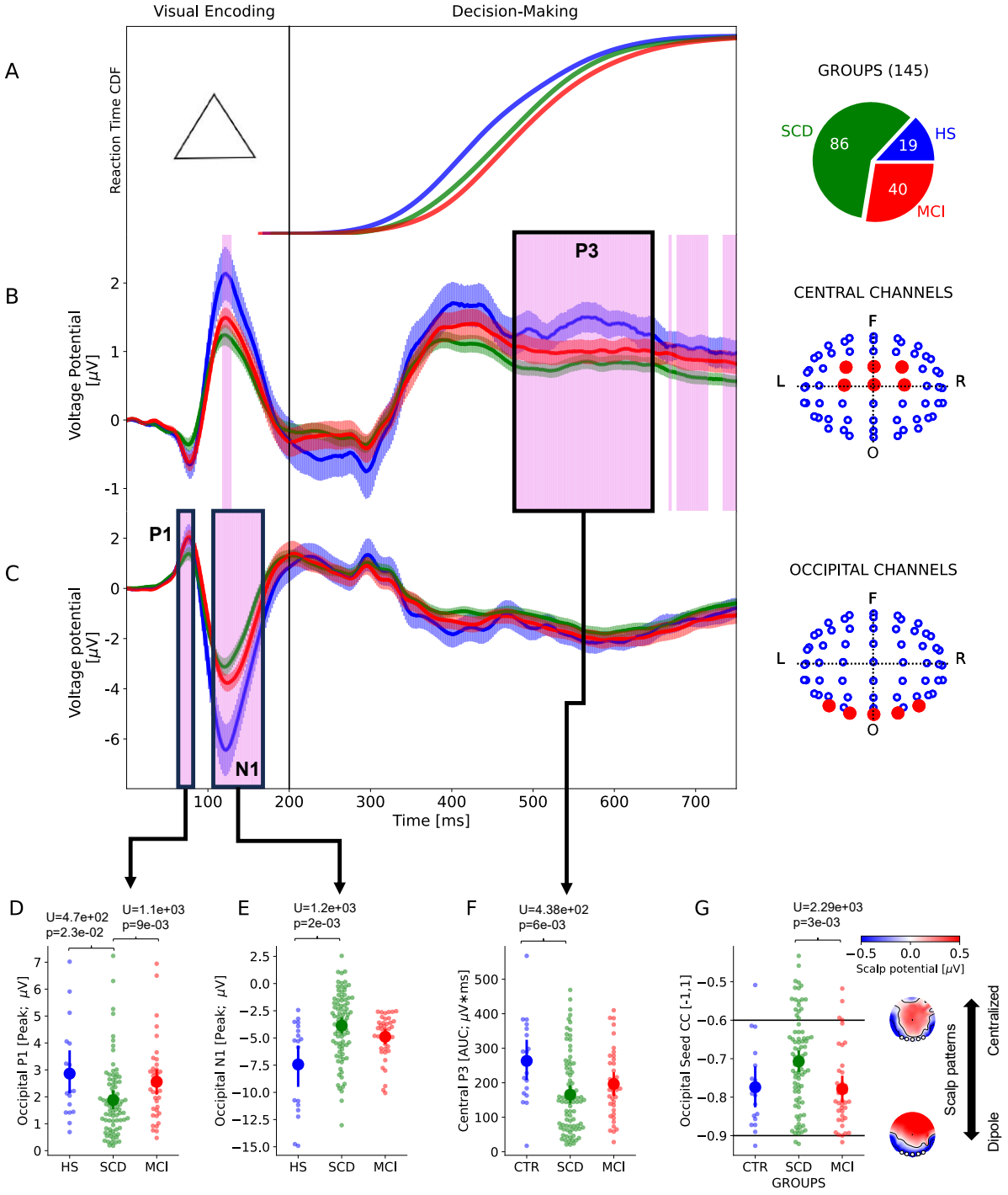

Figure 3. Target stimulus locked ERP wavefronts in patients behaving the 3CVT task. Panel A presents the Cumulative Density Function (CDF) of reaction time, with a triangle denoting the target stimulus presentation within the 0-200ms window. Panels B and C display Event-Related Potentials (ERPs) recorded in central and occipital channels, respectively, with bold lines representing group means and shaded areas indicating standard errors. Violet vertical lines in Panels B and C highlight significant voltage dynamics (p<0.01), particularly associated with the central channel ERP late positive component (P3) and occipital channel ERP early visual components (P1 and N1). Panels D, E, F, and G further illustrate group-specific features: Occipital P1 and N1 peaks, Central P3 integral, and Occipital Seed Correlation Coefficient (Spearman), respectively. Occipital Seed Correlations (Panel G) also shows the average scalp topography in relation to extremes values of correlation (max anticorrelation, i.e., close to -1, associates with dipole voltage patterning on the scalp, while weak anticorrelation, i.e., close to -0.5, associates with centralized voltage patterning on the scalp). U statistics in Panels D-G are significant (p<0.05). Small dots represent individual subject values, while large dots denote the group mean. Abbreviations include HS (healthy controls), SCD (subject cognitive decline), MCI (mild cognitive impairment), and colour coding distinguishes patient groups (SCD in green, MCI in red, and healthy subjects in blue).

Table 2 ERP features extracted from ERP dynamics. Neural features are the peak, integral and latencies of occipital P1 and N1 and central P1, P2 and P3; others are the correlation of the scalp with occipital and central seeds. P-value in bold is <0.05. Features values are indicated with mean and 95% confidence level (CI). Abbreviations: H is the Kruskal-Wallis statistics; Eta-squared is the statistics effect size; HS, healthy controls; SCD, subject cognitive decline; MCI, mild cognitive impairment.

Neural Feature	HS (Mean & CI)	SCD (Mean & CI)	MCI (Mean & CI)	H	p-value	Eta-squared
Occipital N1 (Peak; µV)	-7.44 (-9.29, -5.58)	-3.86 (-4.52, -3.21)	-4.89 (-5.51, -4.27)	1.51E+01	**3.20E-03**	7.70E-01
Occipital Seed CC (-1,1)	-0.77 (-0.83, -0.72)	-0.71 (-0.73, -0.68)	-0.78 (-0.81, -0.75)	1.25E+01	**3.80E-03**	7.58E-01
Occipital P1 (Peak; µV)	2.86 (2.10, 3.63)	1.88 (1.59, 2.16)	2.56 (2.11, 3.00)	1.29E+01	**9.50E-03**	8.77E-01
Occipital N1 (AUC; µV*ms)	280.34 (207.44, 353.23)	161.04 (137.71, 184.37)	187.00 (158.31, 215.68)	1.18E+01	**1.61E-02**	7.82E-01
Occipital P1 (AUC; µV*ms)	34.68 (23.99, 45.36)	22.79 (18.93, 26.64)	31.40 (25.75, 37.05)	1.17E+01	**1.70E-02**	7.62E-01
Central P3 (AUC; µV*ms)	263.28 (208.06, 318.49)	165.53 (141.53, 189.54)	196.39 (165.17, 227.61)	1.19E+01	**2.30E-02**	7.60E-01
Central P3 (Peak; µV)	2.12 (1.76, 2.49)	1.54 (1.36, 1.72)	1.78 (1.54, 2.02)	1.05E+01	**4.83E-02**	8.97E-01
Central P2 (Peak; µV)	2.85 (2.36, 3.33)	2.09 (1.87, 2.32)	2.19 (1.86, 2.52)	9.31E+00	8.55E-02	8.96E-01
Central Seed CC (-1,1)	-0.01 (-0.16, 0.14)	0.03 (-0.04, 0.10)	0.16 (0.06, 0.27)	5.83E+00	1.08E-01	8.75E-01
Central P2 (AUC; µV*ms)	326.38 (261.40, 391.36)	234.56 (203.00, 266.11)	229.82 (189.80, 269.84)	8.03E+00	1.62E-01	7.60E-01
Central P3 (Lat; ms)	557.17 (526.63, 587.70)	553.06 (538.86, 567.25)	560.15 (538.78, 581.52)	5.35E-01	7.27E-01	7.59E-01
Occipital P1 (Lat; ms)	73.49 (70.75, 76.23)	74.02 (72.66, 75.38)	74.80 (72.94, 76.66)	1.06E+00	7.63E-01	7.59E-01
Central P2 (Lat; ms)	420.02 (396.87, 443.17)	409.10 (399.60, 418.60)	426.48 (412.09, 440.88)	3.47E+00	8.06E-01	7.59E-01
Central P1 (Peak; µV)	2.15 (1.51, 2.79)	1.74 (1.50, 1.99)	1.84 (1.54, 2.13)	1.96E+00	8.50E-01	8.97E-01
Central P1 (Lat; ms)	122.26 (119.33, 125.19)	120.44 (118.97, 121.91)	120.15 (118.10, 122.20)	1.39E+00	8.54E-01	7.59E-01
Central P1 (AUC; µV*ms)	32.26 (22.13, 42.40)	25.91 (21.76, 30.06)	26.67 (22.03, 31.30)	1.81E+00	8.88E-01	7.59E-01
Occipital N1 (Lat; ms)	128.53 (122.56, 134.50)	125.53 (122.31, 128.75)	131.98 (126.30, 137.67)	3.76E+00	9.17E-01	7.59E-01

Task performance correlates with amplitude in central scalp EEG potentials

We examined how group categories in ERPs relate to task performance. We focused on F-Measure, combining accuracy and reaction time. Splitting at the median (0.896), we formed two balanced groups: low (n=72) below median, high (n=73) above. Subjects belonging to the high F-Measure category are characterised by higher accuracy (mean=95.3%, std=2.87%; H=8.20, p=4e-03) and shorter reaction times (mean=0.41s, std=0. 04s; H=7.34e+1, p=1.05e-17), compared to subjects in the low F-Measure category, having lower accuracy (mean=91.5%, std=7.35%) and longer reaction time (mean=0.53s, std=0.07s). Reaction time had a smaller p-value than accuracy, indicating F-Measure's focus on decision speed. Both accuracy and reaction time are significant, so we analysed dichotomous F-Measure for overall performance.

ERPs analysed for performance revealed significant time-extended differences, particularly in central channels (FIG4). Decision speed (FIG4A) showed high-performance anticipation by approximately 100ms compared to low performance. Central channels (Fig4B) exhibited significant scalp potential differences during the decision window (~300ms wide). This significant time window (p<0.01), termed Extended Central Potential, includes P2 and P3 potentials. However, occipital channels (Fig4A) did not show significant differences during the encoding phase.

Computation of the integral for Extended Central Potential showed a significant difference between the low and high performance categories (U=1.8e+03; p=2.86e-03; Fig4D). Subsequently, we studied the non-parametric association by means of Spearman-rank correlations between the F-Measure and the integral of the Extended Central Potential. The results showed that in HS (Fig4E) the correlation was positive but not significant (r=0.304; p=6.189e-01), whereas in SCD patients it was positive and significant (r=0.313; p=1.05e-02), and in MCI patients it was positive but not significant (r=0.258; p=3.38e-01). Therefore, the statistical difference observed in the two categories of low and high F-Meausure (Fig. 4D) is mainly drive by SCD patients.

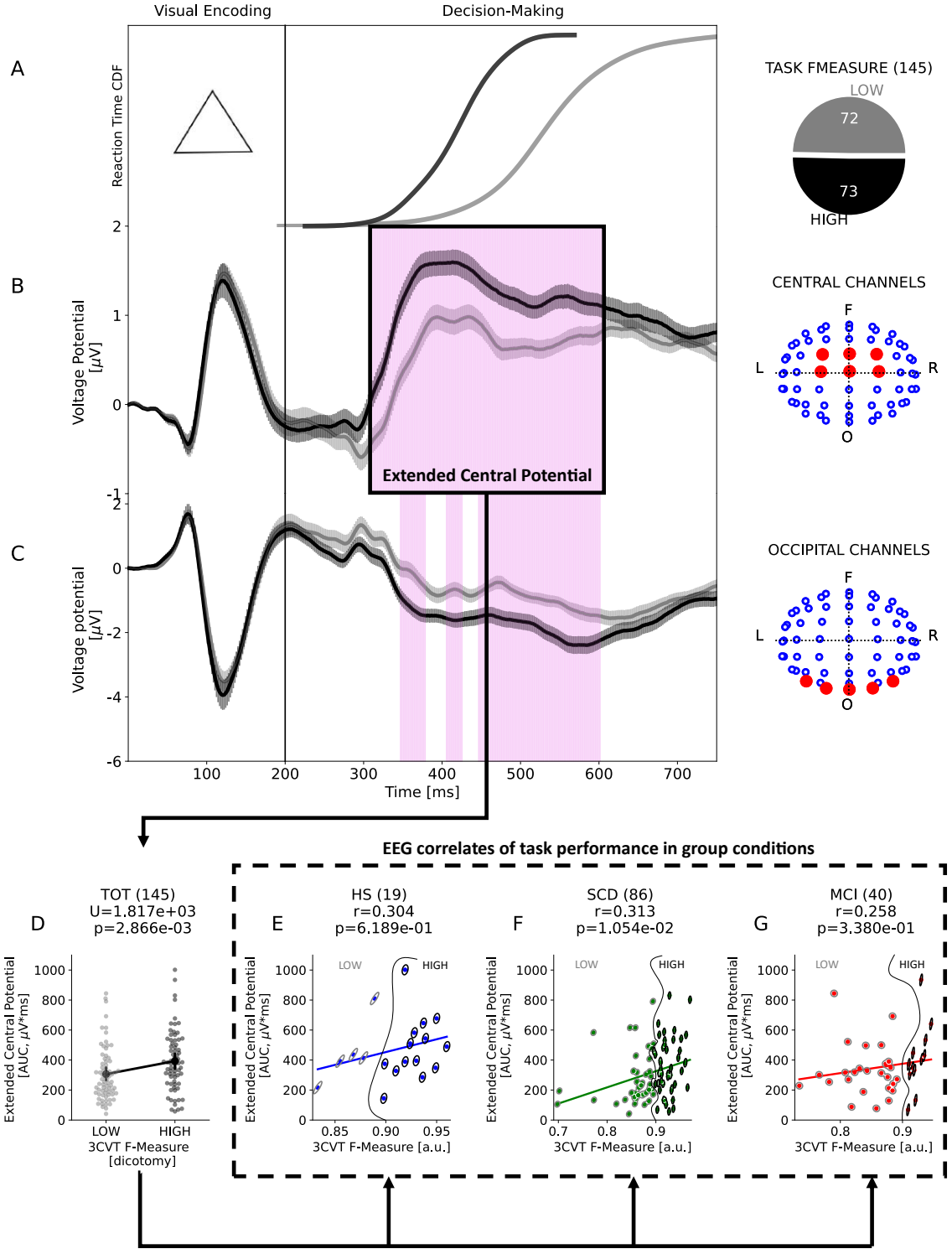

Figure 4. Target stimulus locked ERP wavefronts in performance groups behaving the 3CVT task. Panel A illustrates the Cumulative Density Function (CDF) of reaction time, with a triangle marking the presentation of the target stimulus within the 0-200ms window. Panels B and C showcase Event-Related Potentials (ERPs) recorded in central and occipital channels, respectively. Bold lines represent group means, while shaded areas depict standard errors. Panel D introduces the Extended Central Potentials, differentiated by two performance classes. Panels E-F-G present the Extended Central Potentials relationship with continuous F-Measure for each group condition. Inside scatterplots the circles in grey and black overlaid on scatter points indicates low and high dichotomized F-Meausure. Abbreviations include TOT (all the group conditions), HS (healthy controls), SCD (subject cognitive decline), MCI (mild cognitive impairment).

Ageing check

Since the subjects are of different ages, we asked whether ERP features extracted are affected by effects due to senescence. To this end, we conducted a non-parametric correlation study (Spearman-rank metrics) to highlight possible confounding associations. Analyses showed that the association is only present in HS individuals with the integral of the occipital component N1 (r=0.65; p=8e-03) and the scalp correlation based on occipital seed (r=-0.571; p=4e-02). In contrast, the other features were not significantly associated with age in the groups analysed (see S-Fig4 for statistical details).

Discussion

Study investigated electrophysiological aspects of sustained visual attention in SCD and MCI compared to HS. Anomalies observed in occipital P1 and N1, and central P3 potentials. Non-monotonic ordering highlighted distinctions in SCD compared to HS and MCI. Task performance correlated with central channels' scalp potential intensity, particularly in SCD patients.

These findings support the hypothesis that visual sensory abnormalities characterize SCD and MCI patients to varying degrees. For example, occipital P1 and N1 potentials are thought to represent aspects of visual-attentive processes, including their cost (P1) and benefit (N1) (37–39). Open hypotheses suggest that P1 and N1 may not solely originate from the primary visual cortex, with N1 potentially linked to occipito-parietal/temporal/frontal generators (40), whereas P1 from extra V1 regions (V2,V3, dorsal V4) (41). Therefore, the recorded abnormalities in early visual components between SCD and MCI may indicate a broader visual-attentional impairment specific to these patients.

The most significant neural difference between SCDs and MCIs was EEG scalp correlation with occipital seed, marked by predominantly negative values indicating a basic occipital channels' anticorrelation with others. This results in a dipole topography at the scalp level, characterized by occipital negativity and frontal positivity. SCD patients exhibit less anticorrelation, indicating a reduced dipole effect on the scalp. This occipito-frontal dipole pattern resembles EEG microstate classes C and D (42), which have been associated with AD and non-AD conditions in recent research (43). Future investigations should integrate the theoretical framework of microstates into ERP paradigms in cognitively impaired individuals to explore topographic changes along the occipito-frontal axis.

Assuming a continuous cognitive decline hypothesis (Fig1 in (44)), i.e., according to an increasing gradient of impairment between SCD and MCI patients, an ordering of neural feature values in line with this gradient is to be expected. Instead, a non-monotonic ordering between these features was evidenced, showing greater similarity between controls and MCIs, and thus differentiating SCDs to a greater extent. This non-monotonic characteristic opens questions as to why the electrophysiological correlate does not follow a gradient of change in line with the continuous gradient of cognitive decline. A cause-effect paradigm as a modelling framework (45,46) of pathological AD-type neural degeneration could explain the causal mechanisms underlying the observed non-monotonicity in scalp potentials.

Furthermore, cognitive reserve is recognized for its role in influencing cognitive decline, potentially shielding against dementia symptoms despite existing brain alterations (47). SCD patients exhibited higher proxy scores of cognitive reserve compared to MCI patients, as evidenced by measures of leisure activities and clinical scales. This suggests a potentially greater capacity for brain resilience in supporting cognitive functions among SCD patients.

Patients showed cognitive decline in task performance, with higher performance correlating with increased central scalp recruitment, particularly in SCDs. The Extended Central Potential combines the canonical P2 and P3 central potentials, with P2 reflecting a P300 potential known in the literature as a correlate of decision quality (31). Furthermore, the third positive peak of the central channels (P3), that is also known as late positive potential (LPP), was found suppressed in MCI cohort versus control by Waninger (18), but in right temporo-occipito channels (T4 channel the most significative). Moreover, Waninger et al detected performance correlations with LPP recorded on parietal channels, but during a more working load visual memory test that is the Standardized Image Recognition test (SIR). Therefore, it will be interesting, in future, to extend our analysis by including such a visual memory test to validate prior observations investigating SCD and MCI differences.

Strengths include large sample size, multimodal data (EEG and patient descriptors), and inclusion of CSF markers in a subset. Weaknesses: limited robustness of CSF markers' statistical significance, low healthy subject number (focused on SCD vs. MCI), monocentric study without follow-ups (ongoing in PREVIEW study).

A direct application of the neural features identified in this study is training machine learning algorithms to classify patients based on learned diagnostic categories. Current Alzheimer's disease (AD) biomarkers, such as PET neuroimaging (48) or CSF biomarkers (49), are costly, invasive, and impractical for large-scale use. Our study aims to overcome these limitations by exploring features obtainable through clinical assessments, neuropsychological evaluations, and non-invasive methods like EEG and blood tests. Validating multiple neural features from EEG is crucial to establish their preventive and diagnostic potential.

Acknowledgements

We thank Ahmet Kaymak, Niccolo Meneghetti, Fabio Taddeini, Giovanni Vecchiato, Giacomo Privato and Salvatore Falciglia for their relevant comments which have improved the quality of the research work.

Conflicts

The authors declared no conflict of interest.

Funding Sources

This project was funded by Tuscany Region - PRedicting the EVolution of SubjectIvE Cognitive Decline to Alzheimer's Disease With machine learning - PREVIEW - CUP. D18D20001300002. Funder: Project funded under the National Recovery and Resilience Plan (NRRP), Mission 4 Component 2 Investment 1.3 - Call for tender No. 341 of 15/03/2022 of Italian Ministry of University and Research funded by the European Union – NextGenerationEU Award Number: Project code PE0000006, Concession Decree No. 1553 of 11/10/2022 adopted by the Italian Ministry of University and Research, CUP D93C22000930002, "A multiscale integrated approach to the study of the nervous system in healt and disease" (MNESYS).

Key Words

Subjective Cognitive Decline (SCD); Mild Cognitive Impairment (MCI); EEG; Event-Related Potentials

Bibliography

1. Jessen F, Amariglio RE, van Boxtel M, Breteler M, Ceccaldi M, Chételat G, et al. A conceptual framework for research on subjective cognitive decline in preclinical Alzheimer's disease. Alzheimers Dement. 2014 Nov;10(6):844–52.

2. van Dyck CH, Swanson CJ, Aisen P, Bateman RJ, Chen C, Gee M, et al. Lecanemab in Early Alzheimer's Disease. New England Journal of Medicine. 2023 Jan 5;388(1):9–21.

3. Budd Haeberlein S, Aisen PS, Barkhof F, Chalkias S, Chen T, Cohen S, et al. Two Randomized Phase 3 Studies of Aducanumab in Early Alzheimer's Disease. J Prev Alzheimers Dis. 2022;9(2):197–210.

4. Guest FL, Rahmoune H, Guest PC. Early Diagnosis and Targeted Treatment Strategy for Improved Therapeutic Outcomes in Alzheimer's Disease. In: Guest PC, editor. Reviews on New Drug Targets in Age-Related Disorders [Internet]. Cham: Springer International Publishing; 2020 [cited 2022 Nov 27]. p. 175–91. (Advances in Experimental Medicine and Biology). Available from: https://doi.org/10.1007/978-3-030-42667-5_8

5. Rossini PM, Miraglia F, Vecchio F. Early dementia diagnosis, MCI-to-dementia risk prediction, and the role of machine learning methods for feature extraction from integrated biomarkers, in particular for EEG signal analysis. Alzheimer's & Dementia. 2022;18(12):2699–706.

6. Alexander DM, Arns MW, Paul RH, Rowe DL, Cooper N, Esser AH, et al. Eeg markers for cognitive decline in elderly subjects with subjective memory complaints. J Integr Neurosci. 2006 Mar;05(01):49–74.

7. Babiloni C, Visser PJ, Frisoni G, De Deyn PP, Bresciani L, Jelic V, et al. Cortical sources of resting EEG rhythms in mild cognitive impairment and subjective memory complaint. Neurobiology of Aging. 2010 Oct 1;31(10):1787–98.

8. Paitel ER, Samii MR, Nielson KA. A systematic review of cognitive event-related potentials in mild cognitive impairment and Alzheimer's disease. Behavioural Brain Research. 2021 Jan 1;396:112904.

9. Smailovic U, Koenig T, Kåreholt I, Andersson T, Kramberger MG, Winblad B, et al. Quantitative EEG power and synchronization correlate with Alzheimer's disease CSF biomarkers. Neurobiol Aging. 2018 Mar;63:88–95.

10. Cintra MTG, Ávila RT, Soares TO, Cunha LCM, Silveira KD, de Moraes EN, et al. Increased N200 and P300 latencies in cognitively impaired elderly carrying ApoE ε-4 allele. International Journal of Geriatric Psychiatry. 2018;33(2):e221–7.

11. Morrison C, Rabipour S, Knoefel F, Sheppard C, Taler V. Auditory Event-related Potentials in Mild Cognitive Impairment and Alzheimer's Disease. Current Alzheimer Research. 2018 Jul 1;15(8):702–15.

12. Harding GFA, Wright CE, Orwin A. Primary Presenile Dementia: The Use of the Visual Evoked Potential as a Diagnostic Indicator. The British Journal of Psychiatry. 1985 Nov;147(5):532–9.

13. Kolev V, Yordanova J, Basar-Eroglu C, Basar E. Age effects on visual EEG responses reveal distinct frontal alpha networks. Clinical Neurophysiology. 2002 Jun 1;113(6):901–10.

14. Karamacoska D, Barry RJ, De Blasio FM, Steiner GZ. EEG-ERP dynamics in a visual Continuous Performance Test. International Journal of Psychophysiology. 2019 Dec 1;146:249–60.

15. Chapman RM, Bragdon HR. Evoked Responses to Numerical and Non-Numerical Visual Stimuli while Problem Solving. Nature. 1964 Sep;203(4950):1155–7.

16. Armstrong RA. Alzheimer's Disease and the Eye. Journal of Optometry. 2009 Jan 1;2(3):103–11.

17. Javitt DC, Martinez A, Sehatpour P, Beloborodova A, Habeck C, Gazes Y, et al. Disruption of early visual processing in amyloid-positive healthy individuals and mild cognitive impairment. Alzheimers Res Ther. 2023 Feb 28;15(1):42.

18. Waninger S, Berka C, Meghdadi A, Karic MS, Stevens K, Aguero C, et al. Event-related potentials during sustained attention and memory tasks: Utility as biomarkers for mild cognitive impairment. Alzheimer's & Dementia: Diagnosis, Assessment & Disease Monitoring. 2018 Jan 1;10:452–60.

19. Krasodomska K, Lubiński W, Potemkowski A, Honczarenko K. Pattern electroretinogram (PERG) and pattern visual evoked potential (PVEP) in the early stages of Alzheimer's disease. Doc Ophthalmol. 2010 Oct 1;121(2):111–21.

20. Pollock VE, Schneider LS, Chui HC, Henderson V, Zemansky M, Sloane RB. Visual evoked potentials in dementia: A meta-analysis and empirical study of Alzheimer's disease patients. Biological Psychiatry. 1989 Apr 15;25(8):1003–13.

21. Mangun GR. Neural mechanisms of visual selective attention. Psychophysiology. 1995;32(1):4–18.

22. Mazzeo S, Lassi M, Padiglioni S, Vergani AA, Moschini V, Scarpino M, et al. PRedicting the EVolution of SubjectIvE Cognitive Decline to Alzheimer's Disease With machine learning: the PREVIEW study protocol. BMC Neurology. 2023 Aug 12;23(1):300.

23. Jessen F, Amariglio RE, van Boxtel M, Breteler M, Ceccaldi M, Chételat G, et al. A conceptual framework for research on subjective cognitive decline in preclinical Alzheimer's disease. Alzheimer's & Dementia. 2014;10(6):844–52.

24. Albert MS, DeKosky ST, Dickson D, Dubois B, Feldman HH, Fox NC, et al. The diagnosis of mild cognitive impairment due to Alzheimer's disease: recommendations from the National Institute on Aging-Alzheimer's Association workgroups on diagnostic guidelines for Alzheimer's disease. Alzheimers Dement. 2011 May;7(3):270–9.

25. McKhann GM, Knopman DS, Chertkow H, Hyman BT, Jack CR, Kawas CH, et al. The diagnosis of dementia due to Alzheimer's disease: Recommendations from the National Institute on Aging-Alzheimer's Association workgroups on diagnostic guidelines for Alzheimer's disease. Alzheimer's & Dementia. 2011 May 1;7(3):263–9.

26. Alcolea D, Pegueroles J, Muñoz L, Camacho V, López-Mora D, Fernández-León A, et al. Agreement of amyloid PET and CSF biomarkers for Alzheimer's disease on Lumipulse. Annals of Clinical and Translational Neurology. 2019;6(9):1815–24.

27. Giacomucci G, Mazzeo S, Bagnoli S, Casini M, Padiglioni S, Polito C, et al. Matching Clinical Diagnosis and Amyloid Biomarkers in Alzheimer's Disease and Frontotemporal Dementia. Journal of Personalized Medicine. 2021 Jan;11(1):47.

28. Jack CR, Bennett DA, Blennow K, Carrillo MC, Feldman HH, Frisoni GB, et al. A/T/N: An unbiased descriptive classification scheme for Alzheimer disease biomarkers. Neurology. 2016 Aug 2;87(5):539–47.

29. Stikic M, Johnson RR, Levendowski DJ, Popovic DP, Olmstead RE, Berka C. EEG-derived estimators of present and future cognitive performance. Front Hum Neurosci. 2011;5:70.

30. Danjou P, Viardot G, Maurice D, Garcés P, Wams EJ, Phillips KG, et al. Electrophysiological assessment methodology of sensory processing dysfunction in schizophrenia and dementia of the Alzheimer type. Neuroscience & Biobehavioral Reviews. 2019 Feb 1;97:70–84.

31. Polich J. Updating P300: An integrative theory of P3a and P3b. Clinical Neurophysiology. 2007 Oct 1;118(10):2128–48.

32. Friedman D, Johnson Jr. R. Event-related potential (ERP) studies of memory encoding and retrieval: A selective review. Microscopy Research and Technique. 2000;51(1):6–28.

33. Siems M, Pape AA, Hipp JF, Siegel M. Measuring the cortical correlation structure of spontaneous oscillatory activity with EEG and MEG. NeuroImage. 2016 Apr 1;129:345–55.

34. Spearman C. The Proof and Measurement of Association Between Two Things. East Norwalk, CT, US: Appleton-Century-Crofts; 1961. 45 p. (Studies in individual differences: The search for intelligence).

35. Tan A, Hu L, Tu Y, Chen R, Hung YS, Zhang Z. N1 Magnitude of Auditory Evoked Potentials and Spontaneous Functional Connectivity Between Bilateral Heschl's Gyrus Are Coupled at Inter-individual Level. Brain Connectivity. 2016 Jul;6(6):496–504.

36. Delorme A, Makeig S. EEGLAB: an open source toolbox for analysis of single-trial EEG dynamics including independent component analysis. J Neurosci Methods. 2004 Mar 15;134(1):9–21.

37. Luck SJ, Hillyard SA, Mouloua M, Woldorff MG, Clark VP, Hawkins HL. Effects of spatial cuing on luminance detectability: Psychophysical and electrophysiological evidence for early selection. Journal of Experimental Psychology: Human Perception and Performance. 1994;20:887–904.

38. Luck SJ, Heinze HJ, Mangun GR, Hillyard SA. Visual event-related potentials index focused attention within bilateral stimulus arrays. II. Functional dissociation of P1 and N1 components. Electroencephalography and Clinical Neurophysiology. 1990 Jun 1;75(6):528–42.

39. Mangun GR, Hillyard SA. Modulations of sensory-evoked brain potentials indicate changes in perceptual processing during visual-spatial priming. J Exp Psychol Hum Percept Perform. 1991 Nov;17(4):1057–74.

40. Clark VP, Fan S, Hillyard SA. Identification of early visual evoked potential generators by retinotopic and topographic analyses. Human Brain Mapping. 1994;2(3):170–87.

41. Woldorff M g., Fox P t., Matzke M, Lancaster J l., Veeraswamy S, Zamarripa F, et al. Retinotopic organization of early visual spatial attention effects as revealed by PET and ERPs. Human Brain Mapping. 1997;5(4):280–6.

42. Koenig T, Prichep L, Lehmann D, Sosa PV, Braeker E, Kleinlogel H, et al. Millisecond by Millisecond, Year by Year: Normative EEG Microstates and Developmental Stages. NeuroImage. 2002 May 1;16(1):41–8.

43. Lassi M, Fabbiani C, Mazzeo S, Burali R, Vergani AA, Giacomucci G, et al. Degradation of EEG microstates patterns in subjective cognitive decline and mild cognitive impairment: Early biomarkers along the Alzheimer's Disease continuum? Neuroimage Clin. 2023;38:103407.

44. Sperling RA, Aisen PS, Beckett LA, Bennett DA, Craft S, Fagan AM, et al. Toward defining the preclinical stages of Alzheimer's disease: Recommendations from the National Institute on Aging-Alzheimer's Association workgroups on diagnostic guidelines for Alzheimer's disease. Alzheimer's & Dementia. 2011;7(3):280–92.

45. Lavanga M, Stumme J, Yalcinkaya BH, Fousek J, Jockwitz C, Sheheitli H, et al. The virtual aging brain: a model-driven explanation for cognitive decline in older subjects [Internet]. bioRxiv; 2022 [cited 2023 Jul 13]. p. 2022.02.17.480902. Available from: https://www.biorxiv.org/content/10.1101/2022.02.17.480902v2

46. Amato LG, Vergani AA, Lassi M, Fabbiani C, Mazzeo S, Burali R, et al. Personalized modeling of neurodegeneration determines dementia severity from EEG recordings [Internet]. medRxiv; 2023 [cited 2023 Nov 12]. p. 2023.11.06.23298149. Available from: https://www.medrxiv.org/content/10.1101/2023.11.06.23298149v1

47. Stern Y. Cognitive reserve. Neuropsychologia. 2009 Aug 1;47(10):2015–28.

48. Sabri O, Sabbagh MN, Seibyl J, Barthel H, Akatsu H, Ouchi Y, et al. Florbetaben PET imaging to detect amyloid beta plaques in Alzheimer's disease: phase 3 study. Alzheimers Dement. 2015 Aug;11(8):964–74.

49. Buerger K, Ewers M, Pirttilä T, Zinkowski R, Alafuzoff I, Teipel SJ, et al. CSF phosphorylated tau protein correlates with neocortical neurofibrillary pathology in Alzheimer's disease. Brain. 2006 Nov;129(Pt 11):3035–41.